

## Programmed cell death protein 1/programmed cell death ligand 1 signaling pathway mediated interleukin-10 and bacterial biofilm formation to drug resistance mechanism of pneumoniae meningitis

Chen Ma, Yi Zhang, Jin'e Lei, Jing Zhang, Fang Li, Xiaqin He, Jing Yuan, Wen Li, Wei Chen\*

Department of Laboratory, the First Affiliated Hospital of Xi'an Jiaotong University, Xi'an 710061, Shaanxi Province, China

### ARTICLE INFO

#### Original paper

#### Article history:

Received: February 18, 2023

Accepted: April 06, 2023

Published: April 30, 2023

#### Keywords:

*Pneumococcal meningitis, drug susceptibility test, biofilm, programmed cell death protein 1/ programmed cell death ligand 1 signaling pathway*

### ABSTRACT

It aimed to explore the resistance and biofilm formation characteristics of pneumococcal meningitis (PM) and the mechanism of programmed cell death protein 1/programmed cell death ligand 1 (PD-1/PD-L1) signaling pathway (SPW). Firstly, the drug susceptibility test of 32 *Streptococcus pneumoniae* strains isolated from patients with PM and the biofilm semi-quantitative determination was performed. Then, the PM mouse model was constructed. The differences in brain morphology, blood-brain barrier (BBB) permeability, water content, cytokines such as interferon- $\gamma$  (IFN- $\gamma$ ), interleukin-10 (IL-10), and chemokine C-X-C ligand 10 (CXCL10), and levels of PD-1 and PD-L1 in the normal control (NC), sham operation, PM, and PD-1 antibody (PM + PD-1 Ab) groups were compared and analyzed. The results showed that *Streptococcus pneumoniae* had multidrug resistance, and the thickness of biofilm decreased with the increase of penicillin minimum inhibitory concentration (MIC). Compared with the NC and Sham groups, BBB permeability, water content, levels of IFN- $\gamma$  and IL-10, and PD-1 and PD-L1 were significantly increased in the PM and PM + PD-1 Ab groups, while CXCL10 level was decreased, exhibiting differences with  $P < 0.05$ . Based on the PM group, BBB permeability, water content, levels of IFN- $\gamma$  and CXCL10, and PD-1 and PD-L1 were remarkably decreased in the PM + PD-1 Ab group, while the IL-10 level was observably increased ( $P < 0.05$ ). Therefore, high-MIC penicillin could inhibit the thickness of *Streptococcus pneumoniae* biofilm, while blocking the PD-1/PD-L1 pathway exerted an improving effect on the PM symptoms.

Doi: <http://dx.doi.org/10.14715/cmb/2023.69.4.16>

Copyright: © 2023 by the C.M.B. Association. All rights reserved. 

### Introduction

*Streptococcus pneumoniae* is a globular Gram-positive bacterium, with  $\alpha$  hemolytic characteristics (1). The rate of *Streptococcus pneumoniae*-carrying is high in healthy people, but it is usually a recessive infection (2). *Streptococcus pneumoniae* is a pathogen causing community-acquired infection in children. It can colonize the nasopharynx of children, which causes non-invasive infections such as sinusitis, bronchitis, and pneumonia as well as invasive infections (3). The morbidity and mortality of meningitis resulting from *Streptococcus pneumoniae* are high, and it has become a major cause of bacterial meningitis in children < 5 years old (4). Penicillin is the drug of choice for the treatment of *Streptococcus pneumoniae* infection. However, *Streptococcus pneumoniae* has more than 50% clinical resistance to penicillin, with a minimum inhibitory concentration (MIC)  $\geq 2\mu\text{g/mL}$ , while the insensitivity rate is as high as 75% (5). *Streptococcus pneumoniae* can form a biofilm, which is one of the main factors leading to bacterial insensitivity to antibiotics (6). Besides, the biofilm of drug-susceptible *Streptococcus pneumoniae* is usually thicker than that of drug-resistant strains (7).

Programmed cell death protein 1 (PD-1) is a crucial immunosuppressive molecule in the body's immune sys-

tem and belongs to the CD28 superfamily. The PD-1 target can be applied in the treatment of infection, tumors, and immune diseases (8). Programmed cell death ligand 1 (PD-L1) is covered in the type I transmembrane protein. Inhibition of the PD-1/PD-L1 signaling pathway (SPW) helps promote the oligoclonal amplification of tumor-infiltrating T cells in the body (9). PD-1 antibodies are treating various cancer diseases. Blocking the PD-1/PD-L1 SPW can improve immune cell function and survival rate (10). Infection of *Streptococcus pneumoniae* leads to the imbalance of immune cells in the body (11). Consequently, the PD-1 SPW is involved in the process of the anti-infectious immune response, which is a therapeutic target for immune regulation.

To investigate the characteristics of drug resistance and biofilm formation of pneumococcal meningitis (PM) and the regulation of the PD-1/PD-L1 SPW, the strains isolated from PM patients were collected for the drug susceptibility test and biofilm determination. Subsequently, the model of PM mouse was constructed targeting at therapeutic effect of PD-1 antibody blocking the PD-1/PD-L1 SPW on PM mice. The results were hoped to clarify the mechanism of the PD-1/PD-L1 pathway in the specific anti-infection of *Streptococcus pneumoniae* and to provide new research ideas for preventing and treating PM.

\* Corresponding author. Email: [zhongyan8642900518@163.com](mailto:zhongyan8642900518@163.com)

## Materials and Methods

### Identification and preservation of Streptococcus pneumoniae strains

32 Streptococcus pneumoniae strains isolated from the cerebrospinal fluid (CSF) of patients with PM from the microbial laboratory of the First Affiliated Hospital of Xi'an Jiaotong University from April 2020 to January 2022 were collected as research strains. The standard bacterium for Streptococcus pneumoniae was ATCC49619. The strains were placed in a Columbia culture plate, and the condition was set at 35°C in an incubator containing 5% CO<sub>2</sub>. The colony status was observed after 24 hours of culture. The transparent colony with umbilical concave was selected for the bile dissolution and identification through the Optochin paper method. The dissolved colony with the bacteriostatic ring over 14mm was identified as Streptococcus pneumoniae.

### The drug susceptibility test of Streptococcus pneumoniae

The drug susceptibility test for bacteria was implemented by using the automated bacterial drug susceptibility analyzer combined with disk diffusion and *E* test. The disk diffusion method was adopted to test the resistance to erythromycin, clindamycin, vancomycin, linezolid, trimethoprim-sulfamethoxazole, and levofloxacin. The *E* test was adopted for the resistance to penicillin. Drug susceptibility was evaluated according to the standards established by the American *Clinical and Laboratory Standards Institute* (CLSI). The standard of meningitis was used as the criterion for judging the strain isolated from CSF.

### Biofilm semi-quantitative determination of Streptococcus pneumoniae

The MIC of penicillin against Streptococcus pneumoniae was determined by the agar dilution method. The MIC was divided into 0.05µg/mL, 0.1µg/mL, 0.5µg/mL, 1µg/mL, and 5µg/mL according to the CLSI standard.

Streptococcus pneumoniae was inoculated on the plate of Colombian, and the culture condition was set at 35°C in an incubator containing 5% CO<sub>2</sub>. 24 hours later, the colony status was observed. The colony growing on the plate was transferred to a sterile test tube containing the Todd Hewitt Broth (THB) culture medium by using the inoculation ring. The McFarland concentration was adjusted to 0.5 by the turbidity comparator. 200 µL of the bacterial solution was inoculated into the 96-well plates, and it was cultured in the incubator for 24 h. The colony was washed with phosphate buffer (PBS) 3 times and placed in a 60°C drying box for 1h. 1% crystal violet solution was used to stain for 15min, and the floating color was washed with PBS, with a 15-minute dry. The A value in each well was detected at 570nm. The biological semi-quantitative determination of bacterial strains was performed with the pure THB culture medium as the blank control group.

### Establishment of the model of PM mice

The mice were anesthetized by intraperitoneal injection of 0.4 mL 1.8% tribromoethanol anesthetics. After weighing, the mice were fixed in the prone position on the operating table. Hair was removed along with the mouse head, and a 1.5 cm incision was made in the midline sagittal position. The injection point was taken from the

midpoint of the posterior connection of the bilateral eye sockets and ears. 15µL Streptococcus pneumoniae with a concentration of 1.5×10<sup>8</sup>cfu/mL was injected slowly and evenly through the skull with a microsyringe, which was perpendicular to the plane of the cranial parietal bone. The needle was retained for 1min, and it was slowly withdrawn. Then, the incision was sutured, and the mark was made. The mice were reared in cages at 22±2°C and placed in the 12 h / 12 h day-and-night-alternating animal laboratory, with a free diet.

The weights of mice were recorded at 3 h, 6 h, 12 h, and 24 h after the inoculation. The Loeffler Neurobehavioral scale was adopted to assess mouse behaviors. 0 points represented death, 1 point represented the inability to exercise normally, 2 points represented the inability to turn over normally, 3 points represented the turning time over 5 s, and 4 points represented the inability to turn over within 5 s, with the reduction of the autonomic movement times, and 5 points represented the ability to turn over within 5 s and move normally.

### Grouping of experimental animals

60 BALB/c mice were selected as the subjects. According to the treatment methods, mice were randomly rolled into the normal control (NC) group, sham operation (Sham) group, PM group, and PD-1 antibody (PM + PD-1 Ab) group, with 15 mice in each group. Mice in the NC group were fed normally and underwent any operative treatment. Mice in the Sham group were subjected to the methods given in section 2.5 and were injected slowly with a microsyringe for 3mm before injection. In the PM group, the models of mice were constructed according to the 2.5-section method. In the PM + PD-1 Ab group, the models of mice were established according to the 2.5-section method. After the successful modeling, 100µL 10mg/mL PD-1 antibody was intraperitoneally injected once every 3 days for 4 times.

### HE staining of brain histopathological changes

After anesthesia, the mice in each group were decapitated to take the brain tissue. After it was frozen at -80°C, the tissue was rinsed with isotonic saline and infused with a mixed solution containing 2% paraformaldehyde and 2% polyglutaraldehyde. Then, it was fixed overnight at 4°C and rinsed with PBS. After the tissue was treated by gradient dehydration with 70%, 80%, 95%, 95%, 100%, and 100% ethanol solution, the xylene solution was added for tissue transparency. The tissue was embedded in the paraffin solution for 30min and sectioned into slices with a thickness of 4µm. After the slices were baked in the drying box, the rehydration of tissue was implemented with the xylene and the 100%, 100%, 90%, 80%, and 70% ethanol solutions. It was dyed with hematoxylin solution for 5min and washed with 1% eosin solution for another 5min. After the gradient alcohol dehydration, xylene was added for tissue transparency, and the sheets were sealed with neutral gum. Finally, a light microscope was employed for histological observation.

### Determination of blood-brain barrier (BBB) permeability and water content of brain tissue

Mice in each group were given 1mL/kg 5% Evans blue (EB) solution by tail vein, and the heads were severed for brain tissue. The optical density of brain tissue was mea-

sured by a spectrophotometer. The EB content was determined by the EB standard curve.

After anesthesia, all the heads of the mice were severed, and the brain tissues were taken and weighed (W0). Subsequently, they were baked in a drying box until constant weight (W1). The water content was calculated with  $(W0-W1)/W0 \times 100\%$ .

#### Determination of the levels of interferon- $\gamma$ (IFN- $\gamma$ ), interleukin-10 (IL-10), and chemokine C-X-C ligand 10 (CXCL10) by the enzyme-linked immunosorbent assay (ELISA) method

According to the ELISA kit instruction, the gradient dilution reagent standard samples were obtained, and the standard curves were drawn. After the gradient dilution of the CSF samples from mice, they were incubated at 37°C for 30 min. The solution was discarded, 50  $\mu$ L enzyme-linked reagent was mixed, and they were incubated at the same condition and duration. Then, 50  $\mu$ L chromogenic solutions A and B were added. After the gentle shake, they were incubated at 37°C for 15 min in dark. 50  $\mu$ L stop buffer was added. With blank wells as the controls, the A value was measured at 450nm.

#### Determination of the messenger ribonucleic acid (mRNA) levels of PD-1 and PD-L1 in brain tissues by reverse transcription-quantitative real-time polymerase chain reaction (RT-qPCR)

After anesthesia, the mice were decapitated for the brain tissues which were washed with PBS and frozen at -80°C. The total RNA was extracted according to the RNA extraction Kit, and its concentration and purity were detected. The reverse transcription of the complementary deoxyribonucleic acid (cDNA) was performed according to the instructions of the kit. Quantitative primers of target genes were synthesized by Shanghai Sangon Biotech Co., Ltd. (Table 1). The reaction system was set according to the RT-qPCR kit.  $\beta$ -actin gene was regarded as the internal reference, and the mRNA level of the target gene was subjected to the  $2^{-\Delta\Delta Ct}$  for calculation.

#### Determination of levels of PD-1 and PD-L1 in brain tissues by Western blot method

After anesthesia, the mice were decapitated, and the brain tissues were kept, which were rinsed with PBS and frozen at -80°C. The radio-immunoprecipitation assay (RIPA) buffer was added for cell lysis, and the supernatant was subjected to protein quantification by using the BCA kit. The concentrated gel and the separated gel were prepared, and electrophoresis of the sample was performed. After the membrane was transferred, the sample protein was sealed with a blocking solution containing 5% skim milk for 1h. Mouse monoclonal antibodies PD-1 (1:1000),

PD-L1 (1:1000), and  $\beta$ -actin (1:1000) were added. With the gentle shaking-up, they were incubated at 4°C all night. The horseradish peroxidase (HRP)-labeled goat anti-rabbit IgG secondary antibody (1:10000) was mixed, and then they were processed at 37°C for 90min. After the membrane was washed, the target protein bands were developed according to the ECL chemiluminescence kit, and the gel imager was employed to photograph. ImageJ was employed to determine the gray values of the target protein bands. The relative levels of PD-1 and PD-L1 target proteins were calculated under the  $\beta$ -actin as the internal reference.

#### Methods for statistics

SPSS 19.0 was utilized for data statistics and analysis. Mean  $\pm$  standard deviation ( $\bar{x} \pm sd$ ) was to show how the research results were displayed. A one-way analysis of variance was adopted for comparison between groups. The difference was statistically considerable with  $P < 0.05$ .

#### Results

##### Drug resistance analysis of Streptococcus pneumoniae

The E test of penicillin was performed on 32 strains isolated from PM patients. There were 8 strains with the penicillin-susceptible streptococcus pneumoniae (PSSP) and 24 strains with the penicillin-resistant streptococcus pneumoniae (PRSP). The disk diffusion method was used to analyze the resistance of strains to other drugs (Figure 1). All 24 PRSP strains were resistant to clindamycin and erythromycin but susceptible to levofloxacin, linezolid, and vancomycin. All 8 PSSP strains were susceptible to levofloxacin, linezolid, and vancomycin.

##### Biofilm semi-quantitative analysis of Streptococcus pneumoniae

The A value was used for the semi-quantitative evaluation of the biofilm thickness of Streptococcus pneumoniae.

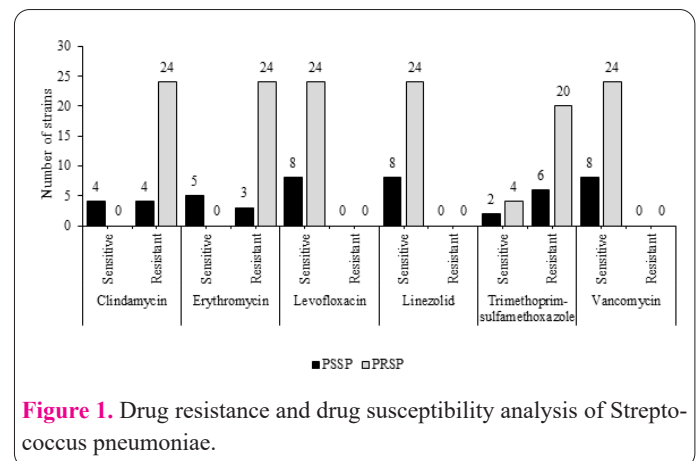


Figure 1. Drug resistance and drug susceptibility analysis of Streptococcus pneumoniae.

Table 1. RT-qPCR primer information.

| Gene           | Primer sequence                        | Primer length (bp) |
|----------------|--|--------------------|
| PD-1           | Forward: 5'-GCACCCCAAGGCAAAAATCG-3'    | 166                |
|                | Reverse: 5'-CAATACAGGGATACCCACTAGGG-3' |                    |
| PD-L1          | Forward: 5'-GCTCCAAAGGACTTGTACGTG-3'   | 238                |
|                | Reverse: 5'-TGATCTGAAGGGCAGCATTTC-3'   |                    |
| $\beta$ -actin | Forward: 5'-GTGACGTTGACATCCGTAAGA-3'   | 245                |
|                | Reverse: 5'-GCCGGACTCATCGTACTCC-3'     |                    |

When A value  $\leq 0.12$ , the bacterial biofilm didn't adhere. When A value  $\geq 0.24$ , the bacterial biofilm adhesion was strong. When A was between 0.12 and 0.24, the adhesion ability of bacterial biofilm was poor. Changes in biofilm A value of *Streptococcus pneumoniae* under the penicillin with different MIC were detected (Figure 2). With the increase of the MIC of penicillin, the A value of *Streptococcus pneumoniae* biofilm gradually decreased. Compared with the MIC of 0.05  $\mu\text{g/mL}$ , the A value of *Streptococcus pneumoniae* biofilm was greatly decreased at the MIC of 0.50  $\mu\text{g/mL}$ , 1.00  $\mu\text{g/mL}$ , and 5.00  $\mu\text{g/mL}$  ( $P < 0.05$ ), while the difference in the A value of *Streptococcus pneumoniae* biofilm at the MIC of 0.10  $\mu\text{g/mL}$  exhibited no significance ( $P > 0.05$ ).

### Changes in weight and neurobehavioral scores of mice after modeling

The weight changes of each animal model at different times after modeling were evaluated (Figure 3). The weights in the NC and Sham groups had little change at different times, while that of the PM group and PM + PD-1 Ab group decreased with the extension of modeling time. No considerable difference was observed in the body weight of subjects from the NC and Sham groups at different times ( $P > 0.05$ ). The weight of mice in the PM and PM + PD-1 Ab groups was notably lower at 6h, 12h, and 24h after modeling ( $P < 0.05$ ). The weight of mice in the PM + PD-1 Ab group was markedly higher based on that in the PM group at 6 h, 12 h, and 24 h after modeling ( $P < 0.05$ ).

Neurobehavioral scores of each group were evaluated at different times after modeling (Figure 4). At different times, the neurobehavioral scores of the NC group and Sham group had little changes and exhibited no great difference ( $P > 0.05$ ). Neurobehavioral scores of the PM groups and PM + PD-1 Ab group were observably lower based on those of the NC group and Sham group at 6h, 12h, and 24h after modeling ( $P < 0.05$ ). The PM group exhibited lower neurobehavioral scores than the PM + PD-1 Ab group were higher at 12h, and 24h after modeling, showing differences with  $P < 0.05$ .

### The difference in brain tissue permeability and water content in each group

The EB content and water content in the brain tissues of each group were detected and compared (Figure 5). There were no considerable differences in Evans Blue content and water content between the NC group and Sham group, so  $P > 0.05$  was applicable. The EB and water contents of brain tissues in the PM group and PM + PD-1 Ab group were evidently higher and showed great differences with those in the NC and Sham groups ( $P < 0.05$ ), while those in the PM + PD-1 Ab group were absolutely lower based on the contents in the PM group, exerting difference with  $P < 0.05$ .

### Brain histopathological changes in each group

The pathological changes in brain tissues were detected by the HE staining (Figure 6). The brain structure of the mice in the NC group and Sham group was normal. In the PM group, many inflammatory cells were exuded, and blood vessels became congested, with the hollowing-out phenomenon of cells. The brain structure of mice in the PM + PD-L1 Ab group was improved in contrast to that

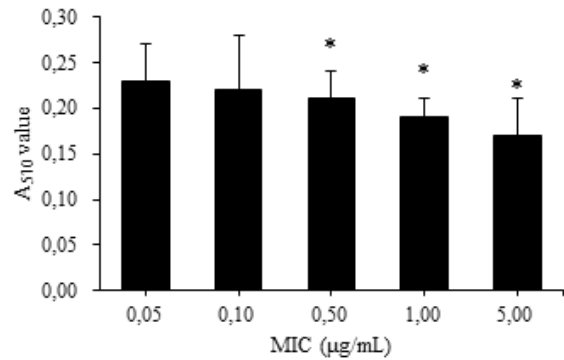


**Figure 2.** Changes in the A value of *Streptococcus pneumoniae* biofilm under the penicillin with different MIC. Note: \* meant that compared with 0.05  $\mu\text{g/mL}$ ,  $P < 0.05$ .

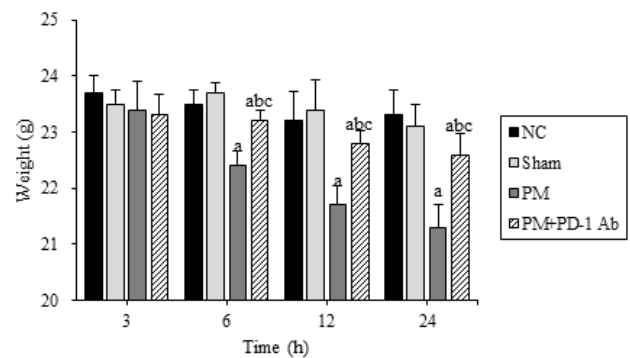


**Figure 3.** The weight changes at different times in each group after modeling. Note: a, b, and c meant  $P < 0.05$  to the NC, Sham, and PM groups, respectively.

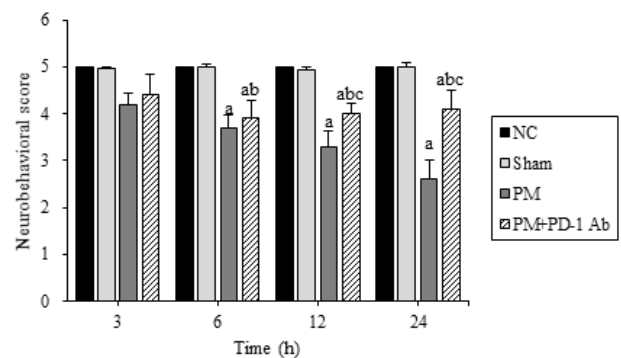


**Figure 4.** Changes in neurobehavioral scores at different times of each group after modeling. Note: a, b, and c meant  $P < 0.05$  to the NC, Sham, and PM groups, respectively.

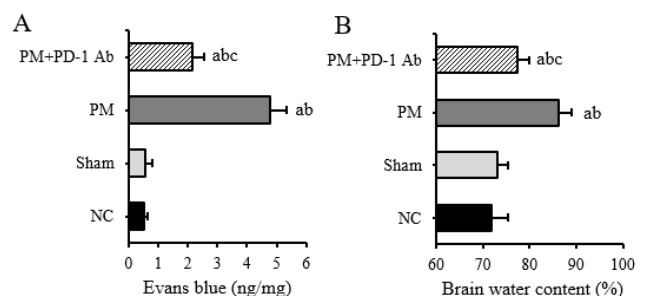


**Figure 5.** Differences in BBB permeability and water content of brain tissue in each group. Note: a, b, and c meant  $P < 0.05$  to the NC, Sham, and PM groups, respectively.

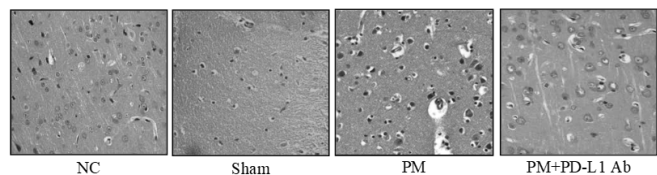


**Figure 6.** HE staining results of brain tissue sections of the mice. Note: the magnification was x 100.

in the PM group, but there were still some problems with inflammatory cell infiltration.

### Differences in the levels of IFN- $\gamma$ , IL-10, and CXCL10 in CSF of each group

Levels of IFN- $\gamma$ , IL-10, and CXCL10 in CSF were detected by ELISA (Figure 7). The differences in IFN- $\gamma$ , IL-10, and CXCL10 levels in CSF between the NC group and Sham group were insignificant ( $P>0.05$ ). The IFN- $\gamma$  and CXCL10 levels in CSF of the PM group and PM + PD-1 Ab group were manifestly lower, while the IL-10 level was higher when they were compared to the NC group and Sham group, exhibiting obvious differences with great significance with  $P<0.05$ . The IFN- $\gamma$  and CXCL10 levels in CSF of the PM + PD-1 Ab group were markedly higher but the IL-10 level was lower based on the values in the PM group, exhibiting great differences ( $P<0.05$ ).

### Differences in the mRNA levels of PD-1 and PD-L1 in brain tissues of each group

mRNA levels of PD-1 and PD-L1 in the brain tissues were illustrated in Figure 8. The differences in the mRNA levels of PD-1 and PD-L1 between the NC group and the Sham group weren't considerable ( $P>0.05$ ). Those in the PM group and PM + PD-1 Ab group were obviously higher than those in the NC group and Sham group ( $P<0.05$ ). The mRNA levels of PD-1 and PD-L1 in the PM + PD-1 Ab group were notably lower than the PM group, presenting great differences with  $P<0.05$ .

### Differences in the PD-1 and PD-L1 levels in brain tissues of each group

Western blot was adopted to detect the contents of PD-1 and PD-L1 in the brain tissues of each group (Figure 9). The PD-1 and PD-L1 levels in the NC group exhibited a not obvious difference from that in the Sham group, so  $P>0.05$  was applicable. Based on the NC and the Sham groups, the PD-1 and PD-L1 protein expression in brain tissues of the PM group and PM + PD-1 Ab group were absolutely higher ( $P<0.05$ ). The PD-1 and PD-L1 expressions in brain tissue of the PM + PD-1 Ab group were remarkably lower based on the values in the PM group, displaying obvious differences with  $P<0.05$ .

## Discussion

*Streptococcus pneumoniae* can cause invasive infections such as meningitis and bloodstream infections in children. Its clinical mortality ranges from 11% to 60%, and 25% to 50% of the surviving children have severe neurological sequelae (12, 13). Currently, the drug resistance of *Streptococcus pneumoniae* is becoming increasingly serious in clinical practice, and its drug resistance rate to penicillin is as high as 60%-88% (14). According

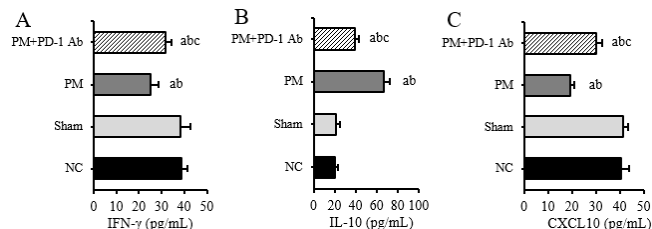


**Figure 7.** Comparison of the differences in IFN- $\gamma$ , IL-10, and CXCL10 levels in each group. (A: IFN- $\gamma$  level; B: IL-10 level; C: CXCL10 level). Note: a, b, and c meant  $P<0.05$  to the NC, Sham, and PM groups, respectively.

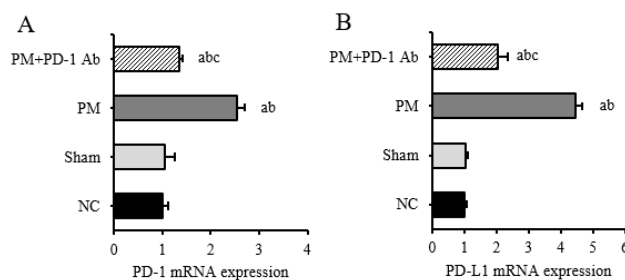


**Figure 8.** Differences in the mRNA levels of PD-1 and PD-L1 in brain tissues of each group. (A: PD-1 mRNA expression; B: PD-L1 mRNA expression). Note: a, b, and c meant  $P<0.05$  to the NC, Sham, and PM groups, respectively.

to this experiment, the resistance rate of CSF isolates from PM children to penicillin was 75%, and that to clindamycin, erythromycin, and trimethoprim-sulfamethoxazole were 87.5%, 84.4%, and 81.3%, respectively. However, the isolates were susceptible to levofloxacin, linezolid, and vancomycin. Hence, levofloxacin, linezolid, and vancomycin could be adopted for the treatment of PM clinically. Besides, biofilm leads to bacterial resistance to antibiotics, but this resistance is reversible and unstable (15). The antibiotic-susceptible *Streptococcus pneumoniae* has thick biofilms (16). The experiment in this work showed that the thickness of *Streptococcus pneumoniae* biofilm decreased with the increase of MIC of penicillin. Nevertheless, the formation of bacterial biofilm is very complex that is affected by many factors (17). Therefore, it needs to be further explored in the future.

The basic pathological changes of meningitis caused by *Streptococcus pneumoniae* include soft meningitis, hyperemia of meningeal vessels, and infiltration of inflammatory cells (18). Presently, the preparation methods for the PM animal models include bacterial inoculation and induction in the nasal cavity, vein, and abdominal cavity (19). Intraventricular bacterial inoculation can effectively avoid BBB and reduce the mortality caused by non-meningitis infection (20). In this experiment, the PM animal model was prepared by the intraventricular injection of *Streptococcus pneumoniae*. The weight and neurobehavioral score of the PM mice were signally lower than that of the normal mice, while the BBB permeability and water content of the brain were markedly higher. Furthermore, there were inflammatory cell infiltration and vascular congestion in the staining of brain tissue sections. It demonstrated that the models were successfully prepared.

Macrophages are a kind of antigen-presenting cells as well as a kind of innate immune cells (21). Macrophages

are the key cells to resist the disease of Streptococcus pneumoniae and other bacteria, whose activation state can be classified into the classic activation M1 type and alternative activation M2 type (22). The M1 type depends on the cell-inflammatory mediators such as IFN- $\gamma$ , TNF- $\alpha$ , and IL-2 to submit antigens, thereby eliminating the pathogens in the body (23). The M2-type activation depends on IL-10 and other inflammatory cytokines to activate inflammatory stimuli and mediate the immune escape of tumors and pathogens. The increase of PD-L1 antibody level helps promote the release of inflammatory factors in the body, thus promoting the transformation of macrophages from M2 to M1 (24, 25). The IFN- $\gamma$  and CXCL10 levels were decreased in the brains of PM mice, while the IL-10 levels were increased according to the results of this experiment. It indicated that the immune function of Th1 and Th2 cells was abnormal in the pathogenesis of PM (26). Nevertheless, after the PD-1 antibody was added, the IFN- $\gamma$  and CXCL10 levels in the brain tissue of the PM mice were increased, while the IL-10 levels were decreased. Also, Meningitis has been studied from cellular and molecular aspects (27-29).

These results indicated that the inhibition of the PD-1/PD-L1 SPW could enhance the immune function of T cells, maintain the immune disorder of Th1/Th2, and achieve the effect of the anti-infection of Streptococcus pneumoniae.

Clinically, Streptococcus pneumoniae in CSF of children with PM showed multi-drug resistance. However, the isolated strains were susceptible to levofloxacin, linezolid, and vancomycin, so these drugs could be selected for the infection treatment. The formation of biofilm of Streptococcus pneumoniae was related to the MIC of antibacterial drugs, but the mechanism of action needed to be further explored. During the occurrence and progression of PM, blocking the PD-1/PD-L1 SPW played a therapeutic role in PM by affecting the activation state of macrophages and the Th1/Th2 type immune response. Nonetheless, regulating PD-1/PD-L1 SPW and the PM process needed to be further investigated. In conclusion, the results of this work could provide new research ideas for the clinical treatment of PM.

## References

- Cillóniz C, Amaro R, Torres A. Pneumococcal vaccination. *Curr Opin Infect Dis* 2016 Apr; 29(2): 187-96. doi: 10.1097/QCO.0000000000000246. PMID: 26779776.
- Holzer L, Hoffman T, Van Kessel DA, Rijkers GT. Pneumococcal vaccination in lung transplant patients. *Expert Rev Vaccines* 2020 Mar; 19(3): 227-234. doi: 10.1080/14760584.2020.1738224. Epub 2020 Mar 11. PMID: 32133883.
- Shah P, Woytanowski JR, Hadeh A, Sockrider M. Pneumococcal (Pneumonia) Vaccines. *Am J Respir Crit Care Med* 2020 May 1; 201(9): P17-P18. doi: 10.1164/rccm.2019P17. PMID: 32356685.
- Koelman DLH, Brouwer MC, van de Beek D. Resurgence of pneumococcal meningitis in Europe and Northern America. *Clin Microbiol Infect* 2020 Feb; 26(2): 199-204. doi: 10.1016/j.cmi.2019.04.032. Epub 2019 May 14. PMID: 31100424.
- Bewersdorf JP, Grandgirard D, Koedel U, Leib SL. Novel and preclinical treatment strategies in pneumococcal meningitis. *Curr Opin Infect Dis* 2018 Feb; 31(1): 85-92. doi: 10.1097/QCO.0000000000000416. PMID: 29095719.
- Wu X, Jacobs NT, Bozio C, Palm P, Lattar SM, Hanke CR, Watson DM, Sakai F, Levin BR, Klugman KP, Vidal JE. Competitive Dominance within Biofilm Consortia Regulates the Relative Distribution of Pneumococcal Nasopharyngeal Density. *Appl Environ Microbiol* 2017 Aug 1; 83(16): e00953-17. doi: 10.1128/AEM.00953-17. PMID: 28576759; PMCID: PMC5541221.
- Yadav MK, Go YY, Chae SW, Park MK, Song JJ. Asian Sand Dust Particles Increased Pneumococcal Biofilm Formation in vitro and Colonization in Human Middle Ear Epithelial Cells and Rat Middle Ear Mucosa. *Front Genet* 2020 Apr 24; 11: 323. doi: 10.3389/fgene.2020.00323. PMID: 32391052; PMCID: PMC7193691.
- Lei Q, Wang D, Sun K, Wang L, Zhang Y. Resistance Mechanisms of Anti-PD1/PDL1 Therapy in Solid Tumors. *Front Cell Dev Biol* 2020 Jul 21; 8: 672. doi: 10.3389/fcell.2020.00672. PMID: 32793604; PMCID: PMC7385189.
- Sun C, Mezzadra R, Schumacher TN. Regulation and Function of the PD-L1 Checkpoint. *Immunity* 2018 Mar 20; 48(3): 434-452. doi: 10.1016/j.immuni.2018.03.014. PMID: 29562194; PMCID: PMC7116507.
- Kwong YL, Chan TSY, Tan D, Kim SJ, Poon LM, Mow B, Khong PL, Loong F, Au-Yeung R, Iqbal J, Phipps C, Tse E. PD1 blockade with pembrolizumab is highly effective in relapsed or refractory NK/T-cell lymphoma failing l-asparaginase. *Blood* 2017 Apr 27; 129(17): 2437-2442. doi: 10.1182/blood-2016-12-756841. Epub 2017 Feb 10. PMID: 28188133.
- Blot M, Jacquier M, Pauchard LA, Rebaud C, Marlin C, Hamelle C, Bataille A, Croisier D, Thomas C, Jalil A, Mirfendereski H, Piroth L, Chavanet P, Bensoussan D, Laroye C, Reppel L, Charles PE. Adverse Mechanical Ventilation and Pneumococcal Pneumonia Induce Immune and Mitochondrial Dysfunctions Mitigated by Mesenchymal Stem Cells in Rabbits. *Anesthesiology* 2022 Feb 1; 136(2): 293-313. doi: 10.1097/ALN.0000000000004083. PMID: 34965287.
- Matanock A, Lee G, Gierke R, Kobayashi M, Leidner A, Pilishvili T. Use of 13-Valent Pneumococcal Conjugate Vaccine and 23-Valent Pneumococcal Polysaccharide Vaccine Among Adults Aged  $\geq 65$  Years: Updated Recommendations of the Advisory Committee on Immunization Practices. *MMWR Morb Mortal Wkly Rep* 2019 Nov 22; 68(46): 1069-1075. doi: 10.15585/mmwr.mm6846a5. Erratum in: *MMWR Morb Mortal Wkly Rep* 2020 Jan 03; 68(5152): 1195. PMID: 31751323; PMCID: PMC6871896.
- Soeters HM, Kambiré D, Sawadogo G, Ouédraogo-Traoré R, Bicaba B, Medah I, Sangaré L, Ouédraogo AS, Ouangraoua S, Yaméogo I, Congo-Ouédraogo M, Ky Ba A, Aké F, Velusamy S, McGee L, Van Beneden C, Whitney CG. Evaluation of pneumococcal meningitis clusters in Burkina Faso and implications for potential reactive vaccination. *Vaccine* 2020 Jul 31; 38(35): 5726-5733. doi: 10.1016/j.vaccine.2020.06.002. Epub 2020 Jun 24. PMID: 32591290; PMCID: PMC7388202.
- Chang B, Tamura K, Fujikura H, Watanabe H, Tanabe Y, Kurohama K, Fujita J, Oshima K, Maruyama T, Abe S, Kasahara K, Nishi J, Kubota T, Kinjo Y, Serizawa Y, Shimbashi R, Fukusumi M, Shimada T, Sunagawa T, Suzuki M, Oishi K; Adult IPD Study Group. Pneumococcal meningitis in adults in 2014-2018 after introduction of pediatric 13-valent pneumococcal conjugate vaccine in Japan. *Sci Rep* 2022 Feb 23; 12(1): 3066. doi: 10.1038/s41598-022-06950-w. PMID: 35197497; PMCID: PMC8866494.
- Dennis EA, Coats MT, Griffin S, Pang B, Briles DE, Crain MJ, Swords WE. Hyperencapsulated mucoid pneumococcal isolates from patients with cystic fibrosis have increased biofilm density and persistence in vivo. *Pathog Dis* 2018 Oct 1; 76(7): fty073. doi: 10.1093/femspd/fty073. PMID: 30265307; PMCID: PMC7191870.
- Mitsuwan W, Wintachai P, Voravuthikunchai SP. Rhodomyrtustolive

- mentosa Leaf Extract and Rhodomyrton Combat Streptococcus pneumoniae Biofilm and Inhibit Invasiveness to Human Lung Epithelial and Enhance Pneumococcal Phagocytosis by Macrophage. *CurrMicrobiol* 2020 Nov; 77(11): 3546-3554. doi: 10.1007/s00284-020-02164-3. Epub 2020 Aug 18. PMID: 32812080.
17. Cuevas RA, Eutsey R, Kadam A, West-Roberts JA, Woolford CA, Mitchell AP, Mason KM, Hiller NL. A novel streptococcal cell-cell communication peptide promotes pneumococcal virulence and biofilm formation. *MolMicrobiol* 2017 Aug; 105(4): 554-571. doi: 10.1111/mmi.13721. Epub 2017 Jun 23. PMID: 28557053; PMCID: PMC5550342.
  18. Taylor A, van der Meer G, Perry D, Best E, Webb R. Recurrent Pneumococcal Meningitis Secondary to NasoethmoidalMeningocele. *Pediatr Infect Dis J* 2020 Feb; 39(2): e17-e19. doi: 10.1097/INF.0000000000002520. PMID: 31876613.
  19. Bello C, Cohen-Salmon M, Van Nhieu GT. A Retro-orbital Sinus Injection Mouse Model to Study Early Events and Reorganization of the Astrocytic Network during Pneumococcal Meningitis. *Bio Protoc* 2021 Dec 5; 11(23): e4242. doi: 10.21769/BioProtoc.4242. PMID: 35005087; PMCID: PMC8678551.
  20. Ruger M, Kipp E, Schubert N, Schroder N, Pufe T, Stope MB, Kipp M, Blume C, Tauber SC, Brandenburg LO. The formyl peptide receptor agonist Ac2-26 alleviates neuroinflammation in a mouse model of pneumococcal meningitis. *J Neuroinflammation* 2020 Oct 29; 17(1): 325. doi: 10.1186/s12974-020-02006-w. PMID: 33121515; PMCID: PMC7596991.
  21. Kloek AT, Seron MV, Schmand B, Tanck MWT, van der Ende A, Brouwer MC, van de Beek D. Individual responsiveness of macrophage migration inhibitory factor predicts long-term cognitive impairment after bacterial meningitis. *ActaNeuropathol-Commun* 2021 Jan 6; 9(1): 4. doi: 10.1186/s40478-020-01100-7. PMID: 33407905; PMCID: PMC7789269.
  22. Lv R, Bao Q, Li Y. Regulation of M1-type and M2-type macrophage polarization in RAW264.7 cells by Galectin-9. *Mol Med Rep* 2017 Dec; 16(6): 9111-9119. doi: 10.3892/mmr.2017.7719. Epub 2017 Oct 4. PMID: 28990062.
  23. Paul S, Chhatar S, Mishra A, Lal G. Natural killer T cell activation increases iNOS+CD206- M1 macrophage and controls the growth of solid tumor. *J Immunother Cancer* 2019 Aug 6; 7(1): 208. doi: 10.1186/s40425-019-0697-7. PMID: 31387637; PMCID: PMC6685184.
  24. Gordon SR, Maute RL, Dulken BW, Hutter G, George BM, McCracken MN, Gupta R, Tsai JM, Sinha R, Corey D, Ring AM, Connolly AJ, Weissman IL. PD-1 expression by tumour-associated macrophages inhibits phagocytosis and tumour immunity. *Nature* 2017 May 25; 545(7655): 495-499. doi: 10.1038/nature22396. Epub 2017 May 17. PMID: 28514441; PMCID: PMC5931375.
  25. Loeuillard E, Yang J, Buckarma E, Wang J, Liu Y, Conboy C, Pavelko KD, Li Y, O'Brien D, Wang C, Graham RP, Smoot RL, Dong H, Ilyas S. Targeting tumor-associated macrophages and granulocytic myeloid-derived suppressor cells augments PD-1 blockade in cholangiocarcinoma. *J Clin Invest* 2020 Oct 1; 130(10): 5380-5396. doi: 10.1172/JCI137110. PMID: 32663198; PMCID: PMC7524481.
  26. Zheng K, Zhu L, Ding Y, Zhang X, Chen N, Liu G, He Q. Serum cytokine profile of pediatric patients with laboratory confirmed pneumococcal meningitis. *J Infect Public Health* 2021 Apr; 14(4): 514-520. doi: 10.1016/j.jiph.2021.01.010. Epub 2021 Jan 19. PMID: 33743374.
  27. Aziziaran Z, Bilal I, Zhong Y, Mahmood A, Roshandel MR. Protective effects of curcumin against naproxen-induced mitochondrial dysfunction in rat kidney tissue. *Cell Mol Biomed Rep* 2021; 1(1): 23-32. doi: 10.55705/cmbr.2021.138879.1001.
  28. Long Y, Du X, Ouyang Z, Zhong J, Zeng Y. Research progress on therapeutic effect and mechanism of hydrocortisone on sepsis. *Cell Mol Biomed Rep* 2023; 3(3): 122-129. doi: 10.55705/cmbr.2023.377524.1090.
  29. Azizi Dargahlou S, Iriti M, Pouresmaeil M, Goh LPW. MicroRNAs; their therapeutic and biomarker properties. *Cell Mol Biomed Rep* 2023; 3(2): 73-88. doi: 10.55705/cmbr.2022.365396.1085.